1 **Title**

2 **Wound-initiated hair regeneration by adhesive and shrinkable materials**

3

4 **Author names**

5 Shoichiro Kokabu[1], Kunikazu Tsuji[2], Ayako Washio[3], Kazumasa Murata[3],

6 Mitsushiro Nakatomi[4], Yusuke Ono[5, 6], Osamu Kaminuma[7], Takuma Matsubara[1]

7

8 **Affiliations**

9 [1]Division of Molecular Signaling and Biochemistry, Kyushu Dental University,

10 Kitakyushu, Fukuoka, 803-8580, Japan; r14kokabu@fa.kyu-dent.ac.jp (S.K.);

11 r15matsubara@fa.kyu-dent.ac.jp (T. M.)

12 [2]Department of Orthopedic Surgery, Tokyo Medical and Dental University, Bunkyo,

13 Tokyo, 113-8519, Japan; tsuji.orj@tmd.ac.jp (K. T.)

14 [3]Division of Endodontics and Restorative Dentistry, Kyushu Dental University,

15 Kitakyushu, Fukuoka, 803-8580, Japan; r05washio@fa.kyu-dent.ac.jp (A. W.);

16 r17murata@fa.kyu-dent.ac.jp (K. M.)

[4]Department of Human, Information and Life Sciences, School of Health Sciences, University of Occupational and Environmental Health, Kitakyushu, Fukuoka, 807-8555, Japan; nktm@health.uoeh-u.ac.jp (M. N.)

[5]Department of Muscle Development and Regeneration, Institute of Molecular Embryology and Genetics (IMEG), Kumamoto University, Kumamoto, 860-0811, Japan; ono-y@kumamoto-u.ac.jp (Y. O.)

[6]Tokyo Metropolitan Institute for Geriatrics and Gerontology, Itabashi, Tokyo, 173-0015, Japan; ono-y@kumamoto-u.ac.jp (Y. O.)

[7]Department of Disease Model, Research Institute of Radiation Biology and Medicine, Hiroshima University, Hiroshima, 734-8551, Japan. okami@hiroshima-u.ac.jp (O. K.)

Abstract

Although there is a global demand for hair regrowth, particularly among middle-aged and older individuals, an effective hair growth technology has not yet been established[1]. Hair follicle neogenesis is restricted to the embryonic period, but hair regeneration accompanied by wound healing has been observed under some conditions[2-4]; however, the underlying mechanisms are unclear. Herein, we demonstrated that creating a wound without dermal defects effectively induced postneonatal hair follicle neogenesis. Separating the epidermis from the dermis by topical application of adhesive and shrinkable materials to mouse skin promoted epidermal regeneration, followed by new hair follicle formation. Hair follicle regeneration, accompanied by the upregulation of related genes, can be induced in mice, including middle-aged and aged mice, regardless of species, sex, skin location, or age. The cycle of the regenerated hair eventually synchronized with that of the surrounding physiological hairs. Our new hair regeneration technique based on reproduction of epidermis–dermis interactions provides a novel means to treat hair loss, including androgenetic alopecia.

Introduction

Globally, there is a strong desire for techniques for hair regrowth among males and females. The global market for alopecia therapy was $7.6 billion in 2020 and is expected to reach $13 billion by 2028[1]. Since natural hair follicle formation is known to occur only during the embryonic period, several attempts to treat alopecia by transplanting hair stem cells and hair follicle organoids have been reported[5-15]. However, there have been reports of postneonatal follicular formation associated with the wound-healing process in rabbits[16], mice[17], and humans[18]. A mouse model for investigating wound-induced hair neogenesis (WIHN) has been developed[2]. However, the detailed mechanisms underlying the initiation of WIHN have not been clarified.

An individual hair is generated in a hair follicle through a single hair cycle[19]. The hair follicle, once formed in the embryonic period, repeats the hair cycle, which consists of the catagen, telogen, and anagen phases, throughout its lifetime. During the development of a hair follicle, the epithelium plunges into the mesenchyme, forming a tubular structure[20]. Epithelial–mesenchymal interactions are essential for initiation, and dermal-mesenchymal interactions predominate during the progression of hair follicle formation[21]. No hair follicles formed from chimeric skin that combined the epidermis of the dorsal skin and the dermis of the plantar area. However, hair follicles formed where

61 the dermis of the dorsal skin and the epidermis of the plantar area were combined[22],
62 suggesting that the mesenchyme-derived dermis plays a key role in achieving
63 postneonatal hair regeneration.

64 We hypothesized that hair follicle neogenesis can be induced under conditions in
65 which the dermis remains intact during the skin regeneration process. Successful skin
66 wound induction without dermal defects by a newly developed procedure involving the
67 application of adhesive and shrinkable materials to the skin promoted hair regeneration
68 accompanied by de novo hair follicle neogenesis at almost 100% probability, even in
69 middle-aged and aged mice. The regenerating hair cycle eventually synchronizes with
70 the surrounding hair cycle.

71

72

Results

Shrink material induces hair regeneration

The dorsal hairs of 5-week-old C57BL/6 mice are known to be in the anagen phase. After the hairs were shaved, the skin color became black because the hairs remained in the hair roots in the skin (Fig. 1a). In contrast, the hairs of 8-week-old mice were in the telogen phase and could be easily removed from their roots by shaving. Therefore, the skin revealed its natural skin color after shaving. After application to the shaved dorsal skin in the telogen phase, 10% pyroxylin solution adhered to the skin and then shrank upon drying. Approximately 2 days after application, a skin wound developed at the site of pyroxylin application. Surprisingly, visible hair growth was observed at the wound site approximately 14 days after application. On approximately day 19, hair growth that was essentially at the same level as that of the original, unshaved hairs in the surrounding skin area, both in terms of length and density, was observed (Fig. 1a).

The hair cycle, including the length and timing of telogen and anagen, varies between the sexes and in mouse species[23,24]. In addition to C57BL/6, C3H/He has been used for wound healing and hair growth research[4,23,24]. The hair cycles of these two mouse strains are different (Fig. 1b; http://www.jslc.co.jp/pdf/mouse/2020/019_C3H_HeNSlc). However, there was no

significant difference in the level or time course of hair regeneration following pyroxylin application between the C57BL/6N and C3H/He mouse strains (Fig. 1a and c) or between male and female mice (data not shown).

The abdominal and limb hair characteristics significantly differ from those of the dorsal hair. The skin of the head and back develops from distinct germ layers during embryonic development[25,26]. Therefore, pyroxylin-induced hair regeneration was examined in these regions of C3H/He mice, which are characterized by a long telogen period and a tightly synchronized hair cycle[23] (Fig. 1b). After the development of wounds by pyroxylin application to the abdomen (Fig. 1d), lower limb (Fig. 1e), and head (Fig. 1f) after shaving, hairs regenerated in all the regions with almost the same time course as that observed in the dorsal skin. However, in addition to the lack of beard regeneration, de novo hair growth was not observed in hairless regions, such as the plantar area, following pyroxylin application (data not shown).

The dose-dependent ability of pyroxylin to induce hair regeneration was examined. Pyroxylin at concentrations greater than 1.25% induced essentially the same level of hair regeneration, although obvious wound and hair regeneration was not observed at concentrations less than 0.625% (Fig. 2a). The effects of adhesion- and shrinkage-related materials other than pyroxylin were examined. The application of

bisphenol A-glycidyl methacrylate (Bis-GMA)-based composite resins with low- or high-shrinkage characteristics, polymethyl methacrylate (PMMA), solvent-based styrene-butadiene rubber, and cyanoacrylates created wounds and induced hair regeneration in the dorsal skin, similar to those observed with pyroxylin treatment. Water-soluble materials such as ethylene-vinyl acetate copolymer emulsions and polyvinyl alcohol aqueous solutions can also induce hair regeneration. However, adaptation of pure liquid components, including MMA + 4-META or MMA alone, did not induce hair regeneration (Fig. 2b). To eliminate the involvement of pure chemical irritation in hair regeneration, we applied high concentrations of acids, such as salicylic acid[27], trichloroacetic acid[28], glycolic acid[29], and lactic acid[30], which are frequently used as chemical peeling reagents, to the skin. No apparent wound or hair regeneration was induced by any type or concentration of acid examined (Fig. 2c).

We next performed histological analysis during pyroxylin-induced wound generation and hair regeneration in the dorsal skin. Three hours after pyroxylin treatment, peeling of the epidermis from the dermis was restricted to the area where pyroxylin was applied (Fig. 3a and b). One day later, the epidermis became necrotic, accompanied by an accumulation of inflammatory cells. On day 2, in addition to the beginning of epidermal regeneration with necrotic old epidermis detachment, invasion

of part of the regenerated epidermis into the dermis was observed. On day 5, the invasion of the epidermis toward the deeper dermis and the generation of new hair follicles and sebaceous glands were detected. On day 9, hair shafts were identified in further-grown new hair follicles (Fig. 3c). Hair placodes, which are located on dermal condensates and represent the primordia of hair follicles, can be identified by alkaline phosphatase (ALP) activity[31]. The hair follicle primordium was indicated in the tips of the newly invaded epidermis by increased ALP activity (Fig. 3d). The expression of hair follicle formation- and neogenesis-related genes such as Sox9[32], Lhx2[32], Bmp7[33], Wnt10b[2], Lef1[2], Sonic hedgehog (Shh)[2] and Gli1[33] gradually increased in the dorsal skin following pyroxylin application, peaked at 9 to 14 days, and then decreased (Fig. 3e). These data suggested that separating the epidermis from the dermis is crucial for activating hair follicle formation- and neogenesis-related genes and resulting in the progression of hair regeneration. We named this novel hair follicle neogenesis process epidermis separation-induced hair neogenesis (ESHN).

ESHN occurs in middle-aged and aged mice

The demand for hair regenerative medicine is increasing in the middle-aged and aged life stages because hair loss is an age-related process[34]. Based on the correlation

145 between mouse and human life spans, 56- and 78-week-old C57BL/6J mice are
146 regarded as middle-aged and aged, respectively[35]. The dorsal hair cycles of 56- and 78-
147 week-old C57BL/6J mice are in the 4th telogen phase[24]. Therefore, we next examined
148 ESHN in these mice. Pyroxylin-induced hair regeneration was observed in 56-week-old
149 mice over the same time course as that observed in 8-week-old mice (Figs. 1a, c and
150 4a). Interestingly, similar to the surrounding original hairs, the regenerated hairs were a
151 mixture of black and gray hairs (Fig. 4b). Hair follicle neogenesis was detected by
152 histological examination (Fig. 4c). ESHN occurred even in 78-week-old mice (Fig. 4d
153 and e).
154
155 ***ESHN synchronizes surrounding hair cycle***
156 We further examined the cycle of hair regeneration following repeated shaving. After
157 the length of the regenerated hairs reached approximately the same level as that of the
158 surrounding hairs on day 19, the regenerated hairs were shaved daily. This process
159 enabled the determination of the hair cycle based on the skin color. The black color of
160 the hair regeneration area after shaving on day 19 gradually faded with each subsequent
161 shaving. By the 25th day, the color became almost indistinguishable from the
162 surrounding skin color (Fig. 5a). Corresponding to the skin color alteration, long hair

follicles in an anagen phase with high density were observed in the dorsal skin on day 19. Following repeated daily shaving, the length and density of the follicles tended to decrease, suggesting a transition to the catagen phase. After 7 repeated shavings on day 25, the follicles almost completely entered the telogen phase (Fig. 5b). The hair regeneration process following repeated pyroxylin treatment was examined. Pyroxylin was reapplied to the area where ESHN once occurred during the telogen phase. Hair regeneration was induced in the second pyroxylin application area at the same level as that in the first application area. Essentially, the same level of hair regeneration was also evoked by the third pyroxylin application (Fig. 5c). When ESHN was induced in 4-week-old C3H/He mice that were in the first physiological telogen phase, we observed hair growth two weeks prior to the beginning of the first physiological anagen phase. Following the start of the first physiological anagen phase at approximately day 17, the hair also began to grow from the shaved area without ESHN induction. Based on the skin color after daily shaving from days 20 to 32, the hair cycle in the area of ESHN induction seemed to enter the telogen phase earlier than that in the area retaining the physiological hair cycle. However, the difference mostly disappeared at approximately day 90. Thus, the cycle of ESHN-induced hairs eventually synchronized with that of the surrounding physiological hairs during the second anagen phase (Fig. 5d).

Discussion

In this study, we developed a new technique for inducing hair follicle neogenesis in postneonatal mice. The simple application of adhesive and shrinkable materials to the skin to create a wound without dermal damage initiated the regeneration of hairs with a normal hair cycle even in middle-aged and aged mice.

Based on previous observations showing hair follicle formation during the wound-healing process in the skin of several species[16-18], Ito et al. developed a mouse model of WIHN[2]. When a full-thickness excision of a certain size was created on the dorsal skin of mice in the first or second telogen phase, hair follicle neogenesis occurred in the center of the wound healing area within 2 weeks, and visible hair growth was observed after approximately 4 weeks[2]. The contribution of Wnt signaling to WIHN was further elucidated. Several procedures for follicular regeneration without creating wounds have also been reported. Gat et al. reported that mice expressing stabilized β-catenin controlled by an epidermal promoter undergo a process resembling de novo hair morphogenesis[36]. Essentially, the same results were reported by Lo Celso et al., although both mentioned tumorigenesis based on the maintained activation of Wnt/β-catenin signaling[36,37]. The activation of Hedgehog signaling in adjacent epithelial and stromal cells induces new hair follicle and tumor formation[38].

Several signaling cascades responsible for postneonatal hair formation have been suggested from these previous studies. However, the key event triggering hair follicle neogenesis has still not been identified even in the WIHN model. To explore the black box, we focused on epithelial-mesenchymal interactions. The hair follicle, along with teeth, sweat glands, mammary glands, and salivary glands, is classified as an ectodermal organ. These organs are formed via epithelial–mesenchymal interactions. In particular, mesenchymal cells initiate the organ fate-determining process[21,39]. The initial signal arising from the dermis causes the formation of fair follicles during embryogenesis[40]. Therefore, we hypothesized that the mesenchyme-derived dermis, which remains intact during wound healing, retains the information necessary to initiate hair follicle formation. This hypothesis was proven, at least in part, by our present study demonstrating hair follicle formation following the regeneration of epithelium-derived epidermis above the intact dermis. Yang et al. demonstrated hair follicle neogenesis by artificial dermis transplantation after the creation of a full-thickness skin defect of a size that would not normally trigger WIHN[4], further supporting our results and hypothesis. The ESHN we established in this study might mimic the follicle formation process during embryogenesis.

Our ESHN procedure has several advantages compared to the previous WIHN

model[2-4]. Thus, hair regeneration could be induced simultaneously in almost all the mice examined in short periods. ESHN can be induced multiple times in the skin during the telogen phase. ESHN potentially contributes to the development of hair follicle regenerative methods, e.g., in combination with microsurgery or laser procedures by which the epidermis layer alone can be removed. A new lineage tracking system that enables the identification of the origin of new hair follicles may be helpful to achieve this goal. Organ regeneration procedures based on epithelial-mesenchymal interactions may also be applied to generate regenerative medicines for other ectodermal organs, such as teeth and some glands.

For development of hair follicle regenerative medicine, it is also important to understand the hair cycle process in middle-aged and aged skin environments. Like all other organs, age-related alterations occur in the skin. For example, aged skin is characterized by atrophy (thinning), fragility, dyspigmentation and delayed wound healing[41-43]. In addition, senescent skin cells accumulate progressively with age and impact skin structure and function[44]. During the hair cycle, as the anagen phase gradually shortens, many hair follicles that go through the catagen phase tend to remain in the telogen phase due to aging[45]. This alteration is the main cause of age-related thinning and hair loss, including androgenetic alopecia. In the mouse model of WIHN

235 established by Ito et al., hair follicle neogenesis was inducible only in 7- to 8-week-old
236 or younger mice[2]. However, our present findings demonstrated ESHN not only in young
237 mice but also in middle-aged and aged mice. Moreover, ESHN actively elicited the
238 transition of the hair cycle to the anagen phase from the telogen phase. Although further
239 investigation into the detailed molecular mechanisms underlying the active telogen–
240 anagen transition, e.g., by employing spatial transcriptome analysis, is needed, the
241 results strongly suggested that the hair cycle, even under aged conditions, is regulated
242 independently of other age-related alterations observed in the skin. The ESHN-based
243 active hair cycle transition system is promising for the development of hair growth
244 drugs with novel mechanisms useful even in aged humans.

245

246 **References**

247 1. Castro, A. R., Portinha, C. & Logarinho, E. The booming business of hair loss.
248 *Trends Biotechnol* **41**, 731-735 (2023).
249 2. Ito, M. *et al.* Wnt-dependent de novo hair follicle regeneration in adult mouse
250 skin after wounding. *Nature* **447**, 316-320 (2007).
251 3. Harn, H. I. *et al.* Symmetry breaking of tissue mechanics in wound induced hair
252 follicle regeneration of laboratory and spiny mice. *Nat Commun* **12**, 2595
253 (2021).
254 4. Yang, Y. *et al.* Tracing immune cells around biomaterials with spatial anchors
255 during large-scale wound regeneration. *Nat Commun* **14**, 5995 (2023).
256 5. Kageyama, T. *et al.* Reprogramming of three-dimensional microenvironments
257 for in vitro hair follicle induction. *Sci Adv* **8**, eadd4603 (2022).
258 6. Lee, J. *et al.* Hair-bearing human skin generated entirely from pluripotent stem

cells. *Nature* **582**, 399-404 (2020).

7. Lee, J. *et al.* Hair Follicle Development in Mouse Pluripotent Stem Cell-Derived Skin Organoids. *Cell Rep* **22**, 242-254 (2018).
8. Asakawa, K. *et al.* Hair organ regeneration via the bioengineered hair follicular unit transplantation. *Sci Rep* **2**, 424 (2012).
9. Chuong, C. M., Cotsarelis, G. & Stenn, K. Defining hair follicles in the age of stem cell bioengineering. *J Invest Dermatol* **127**, 2098-2100 (2007).
10. Ehama, R. *et al.* Hair follicle regeneration using grafted rodent and human cells. *J Invest Dermatol* **127**, 2106-2115 (2007).
11. Ikeda, E. *et al.* Fully functional bioengineered tooth replacement as an organ replacement therapy. *Proc Natl Acad Sci U S A* **106**, 13475-13480 (2009).
12. Nakao, K. *et al.* The development of a bioengineered organ germ method. *Nat Methods* **4**, 227-230 (2007).
13. Takagi, R. *et al.* Bioengineering a 3D integumentary organ system from iPS cells using an in vivo transplantation model. *Sci Adv* **2**, e1500887 (2016).
14. Toyoshima, K. E. *et al.* Fully functional hair follicle regeneration through the rearrangement of stem cells and their niches. *Nat Commun* **3**, 784 (2012).
15. Zheng, Y. *et al.* Organogenesis from dissociated cells: generation of mature cycling hair follicles from skin-derived cells. *J Invest Dermatol* **124**, 867-876 (2005).
16. Breedis, C. Regeneration of hair follicles and sebaceous glands from the epithelium of scars in the rabbit. *Cancer Res* **14**, 575-579 (1954).
17. Lacassagne, A. & Latarjet, R. Action of methylcholanthrene on certain scars of the skin in mice. *Cancer Res* **6**, 183-188 (1946).
18. Kligman, A. M. & Strauss, J. S. The formation of vellus hair follicles from human adult epidermis. *J Invest Dermatol* **27**, 19-23 (1956).
19. Kimura-Ueki, M. *et al.* Hair cycle resting phase is regulated by cyclic epithelial FGF18 signaling. *J Invest Dermatol* **132**, 1338-1345 (2012).
20. Pispa, J. & Thesleff, I. Mechanisms of ectodermal organogenesis. *Dev Biol* **262**, 195-205 (2003).
21. Millar, S. E. Molecular mechanisms regulating hair follicle development. *J Invest Dermatol* **118**, 216-225 (2002).
22. Kollar, E. J. The induction of hair follicles by embryonic dermal papillae. *J Invest Dermatol* **55**, 374-378 (1970).
23. Silver, A. F., Chase, H. B. & Potten, C. S. Melanocyte precursor cells in the hair follicle germ during the dormat stage (telogen). *Experientia* **25**, 299-301 (1969).

24. Choi, S. *et al.* Corticosterone inhibits GAS6 to govern hair follicle stem-cell quiescence. *Nature* **592**, 428-432 (2021).
25. Fernandes, K. J. *et al.* A dermal niche for multipotent adult skin-derived precursor cells. *Nat Cell Biol* **6**, 1082-1093 (2004).
26. Jinno, H. *et al.* Convergent genesis of an adult neural crest-like dermal stem cell from distinct developmental origins. *Stem Cells* **28**, 2027-2040 (2010).
27. Zander, E. & Weisman, S. Treatment of acne vulgaris with salicylic acid pads. *Clin Ther* **14**, 247-253 (1992).
28. Chun, E. Y., Lee, J. B. & Lee, K. H. Focal trichloroacetic acid peel method for benign pigmented lesions in dark-skinned patients. *Dermatol Surg* **30**, 512-516; discussion 516 (2004).
29. Erbagci, Z. & Akcali, C. Biweekly serial glycolic acid peels vs. long-term daily use of topical low-strength glycolic acid in the treatment of atrophic acne scars. *Int J Dermatol* **39**, 789-794 (2000).
30. Sharquie, K. E., Al-Tikreety, M. M. & Al-Mashhadani, S. A. Lactic acid chemical peels as a new therapeutic modality in melasma in comparison to Jessner's solution chemical peels. *Dermatol Surg* **32**, 1429-1436 (2006).
31. Paus, R. *et al.* A comprehensive guide for the recognition and classification of distinct stages of hair follicle morphogenesis. *J Invest Dermatol* **113**, 523-532 (1999).
32. Morita, R. *et al.* Tracing the origin of hair follicle stem cells. *Nature* **594**, 547-552 (2021).
33. Lim, C. H. *et al.* Hedgehog stimulates hair follicle neogenesis by creating inductive dermis during murine skin wound healing. *Nat Commun* **9**, 4903 (2018).
34. Jablonski, N. G. The naked truth. *Sci Am* **302**, 42-49 (2010).
35. Flurkey, K., Currer, J. M. & Harrison, D.E. Chapter 20 - Mouse Models in Aging Research. *Mouse Models in Aging Research* **3**, 637-672 (eds Fox, J. G. et al.) (Academic Press, 2007).
36. Gat, U., DasGupta, R., Degenstein, L. & Fuchs, E. De Novo hair follicle morphogenesis and hair tumors in mice expressing a truncated beta-catenin in skin. *Cell* **95**, 605-614 (1998).
37. Lo Celso, C., Prowse, D. M. & Watt, F. M. Transient activation of beta-catenin signalling in adult mouse epidermis is sufficient to induce new hair follicles but continuous activation is required to maintain hair follicle tumours. *Development* **131**, 1787-1799 (2004).

38. Sun, X. *et al.* Coordinated hedgehog signaling induces new hair follicles in adult skin. *Elife* **9**, 46756 (2020).
39. Saito, K. *et al.* Sox21 Regulates Anapc10 Expression and Determines the Fate of Ectodermal Organ. *iScience* **23**, 101329 (2020).
40. Hardy, M. H. The secret life of the hair follicle. *Trends Genet* **8**, 55-61 (1992).
41. Kurban, R. S. & Bhawan, J. Histologic changes in skin associated with aging. *J Dermatol Surg Oncol* **16**, 908-914 (1990).
42. Farage, M. A., Miller, K. W. & Maibach, H. I. *Textbook of aging skin* (Springer, 2010)
43. Gosain, A. & DiPietro, L. A. Aging and wound healing. *World J Surg* **28**, 321-326 (2004).
44. Franco, A. C., Aveleira, C. & Cavadas, C. Skin senescence: mechanisms and impact on whole-body aging. *Trends Mol Med* **28**, 97-109 (2022).
45. Drake, L. A. *et al.* Guidelines of care for the use of topical glucocorticosteroids. American Academy of Dermatology. *J Am Acad Dermatol* **35**, 615-619 (1996).

Figure legends

Fig. 1. Pyroxylin induces skin wounds followed by hair regeneration.

(a) Ten percent pyroxylin solution was applied to the dorsal skin of 5- and 8-week-old C57BL/6N female mice after shaving (yellow arrowhead). Representative photos of 5-week-old mice on day 2 and 8-week-old mice on days 0, 2, 14 and 19 after shaving are shown. (b) The schematics represent the hair cycle of C57BL/6N or C3H/He female mice, as previously reported. (c) Pyroxylin was applied to the dorsal skin of 8-week-old C3H/He, BALB/c, ddY, DBA/2, and NC/Nga mice after shaving (yellow arrowhead). Representative photos on days 0, 2, 14, and 19 are shown. (d-f) Pyroxylin was applied to the skin of the abdomen (d), lower leg (e), and head (f) after shaving (yellow

arrowhead). Representative photos on days 0, 2, 14, and/or 19 are shown. (a-f) All mice examined exhibited the same trend (n=6).

Fig. 2. Hair regeneration is induced in the skin by the application of adhesive and shrinkable materials.

(a) Zero (ethanol: diethyl ether = 1:1 weight), 0.625, 1.25, 2.5, 5, or 10% pyroxylin solution was applied (yellow arrowhead) to the dorsal skin of 8-week-old C3H/He mice after shaving. Representative photos on days 0, 2, 14, and 19 are shown. (b and c) Low- or high-shrinkage light-activated Bis-GMA-based composite resins (L-LABGCR or H-LABGCR), PMMA, SSBR, MMA, MMA + 4-META, PA, EVACE, and cyanoacrylates (b). After shaving, 35% salicylic acid solution, 20% or 50% trichloroacetic acid solution, 35% or 70% glycolic acid solution, and 35% lactic acid solution (c) were applied to the dorsal skin. Representative photos of three independent experiments are shown.

Fig. 3. Hair follicle neogenesis following the separation of the epidermis and dermis.

(a and b) Representative H&E staining images of wounds on dorsal back skin 3 hours after pyroxylin application (a) and a corresponding magnified image (b) are shown. (c) Representative H&E staining images of dorsal back skin wounds on days 0, 1, 2, 5, and

9 are shown. The yellow and red dotted lines indicate the necrotic epidermis and growing panicles, respectively. (d) Representative H&E staining (left) and ALP activity staining (right) images of wounds on the dorsal back skin on days 2 or 5 are shown. The left and right images are consecutive specimens. The arrowhead indicates the ALP activity-positive area. The yellow and blue dotted lines indicate growing panicles and hair follicles, respectively. Representative images (a-d) with the same trend from 6 individual mice are shown. (a-d) Scale bars indicate 100 μm. (e) mRNA levels of Sox9, Lhx2, Bmp7, Wnt10b, Lef1, Shh, and Gli1 in the dorsal back skin of wounds on 2, 5, 7, 9, or 14 were determined by real-time PCR. The data are expressed as the mean ± SEM of triplicate measurements. $^{**}p < 0.01$, compared with the day 2 sample. Essentially, the same results were obtained from three independent mice.

Fig. 4. ESHN in middle-aged and aged mice.

(a-e) Ten percent pyroxylin solution was applied (yellow arrowhead) to the dorsal hair of middle-aged (a-c) and aged (d, e) C57BL/6J male mice after shaving. (a, d) Representative photos on days 0, 2, and 14 are shown. (b, d) Representative photos of original resided hairs (left) and regenerated hairs (right: on day 20) observed under stereomicroscopy are shown. (c, e) Representative H&E staining images of dorsal back skin wounds on day 5 are shown. Scale bars indicate 100 μm. (a-e) All mice examined

393 exhibited the same trend (n=6).

394 **Fig. 5. Hair cycle synchronization in regenerated and surrounding hairs.**

395 (a) Ten percent pyroxylin solution was applied to the dorsal hair of 8-week-old C3H/He
396 mice after shaving. Beginning on day 19, the regenerated hairs were shaved every day.
397 Representative photos on days 19, 22, and 25 are shown. (b) Representative H&E
398 staining images of dorsal back skin wounds on days 19, 22, and 25 are shown. (c) Ten
399 percent pyroxylin solution was applied to the dorsal hair of 8-week-old C3H/He mice
400 after shaving (green arrow). The photos are shown on day 0, 19, or 25 (1st ESHN). A
401 10% pyroxylin solution was also applied at the same location for the first time (2nd
402 time; red arrow). The photos are shown on day 0, 19, or 25 (2nd ESHN). Again, a 10%
403 pyroxylin solution was applied to the same place for the 2nd time (3rd time; blue
404 arrow). The photos are shown on day 0, 19, or 25 (3rd ESHN). (d) Pyroxylin was
405 applied to the dorsal hair of 4-week-old C3H/He mice after shaving (yellow arrowhead).
406 Beginning on day 20, the regenerated hair was shaved every day for 2 weeks.
407 Representative photos on days 0, 6, 14, 17, 20, 22, 25, 32, and 90 are shown. All mice
408 examined exhibited the same trend (n=6).

409

410 **Methods**

411 ***Animals***

412 Mice were purchased from Japan SLC, Inc. (Hamamatsu, Japan). The mouse strains
413 used were BALB/c, ddY, DBA/2, NC/Nga, C3H/He, NOD/SCID, and C57BL/6N. We
414 also purchased 56- or 78-week-old C57BL/6J mice from The Jackson Laboratory Japan,
415 Inc. (Yokohama, Japan). All studies were performed in accordance with the guidelines
416 of and approved by the Experimental Animal Care and Use Committee of Kyushu
417 Dental University (approval numbers #22-004, #22-020, #22-022, #23-006, #23-014,
418 and #23-016).

419 ***Adhesive and shrinkable materials***

420 Various concentrations of pyroxylin solution (ethanol: diethyl ether = 1:1 wight)
421 (FUJIFILM Wako Chemicals, Osaka, Japan)**,** hydrosoluble ethylene-vinyl acetate
422 copolymer emulsion (EVACE, ALTEC, Shiga, Japan), polyvinyl alcohol aqueous
423 solution (PA, Yamato Co., Ltd., Tokyo, Japan), cyanoacrylates (Toagosei Company,
424 Limited, Tokyo, Japan), solvent-based styrene butadiene rubber (SSBR, Cemedine Co.,
425 Ltd., Tokyo, Japan), light-activated bis-GMA-based composite resin (LABGCR,
426 Nippon Shika Yakuin Co., Ltd., Shimonoseki, Japan), methyl methacrylate (MMA,
427 Shofu, Inc., Kyoto, Japan), 4-methacryloxy ethyl trimelitate anhydride (4-META, Sun
428 Medical Company), and polymethyl methacrylate (PMMA) powder (Sun Medical

Company, Ltd., Shiga, Japan) mixed with MMA + 4META were used for dorsal application. PMMA powder was mixed with MMA and 4-META to initiate polymerization immediately before dorsal application. Salicylic acid (FUJIFILM Wako Chemicals), trichloroacetic acid (FUJIFILM Wako Chemicals), glycolic acid (FUJIFILM Wako Chemicals), and lactic acid (FUJIFILM Wako Chemicals) diluted in polyethylene glycol 300 (FUJIFILM Wako Chemicals) were also used.

Material application to the skin

Mice were anesthetized under general anesthesia using a triad of anesthetics: medetomidine (Nippon Zenyaku Kogyo Co., Ltd., Fukushima, Japan) (0.75 mg/kg), midazolam (Astellas Pharma, Inc., Tokyo, Japan) (4 mg/kg), and butorphanol (Meiji Seika Pharma Co., Pharma, Inc., Tokyo, Japan) (5 mg/kg)[46-48]. The dorsal hair was shaved using clippers, and materials were applied as 7-8-mm-diameter circular sites. Light-activated bis-GMA-based composite resins were polymerized by light-emitting diode irradiation immediately following application.

Quantitative real-time PCR

Total RNA was isolated from the skin tissues using a FastGeneTM RNA Basic Kit (Nippon Genetics, Tokyo, Japan) and reverse-transcribed into cDNA using a high-capacity cDNA reverse transcription kit (Applied Biosystems, Waltham, MA, USA).

447 SYBR Green-based quantitative polymerase chain reaction (qPCR) was performed
448 using PowerUp SYBR (Thermo Fisher Scientific, Waltham, MA, USA) and the
449 QuantStudio 3 Real-Time PCR System (Thermo Fisher Scientific). Relative
450 quantification was performed by the *Δ*CT method using *Gapdh* and *Tbp* as the
451 housekeeping genes for normalization. Primer information was provided as supramental
452 information.

453 ***Histopathological examination***

454 Skin samples were fixed with 4% paraformaldehyde (Nacalai Tesque, Inc., Kyoto,
455 Japan) in PBS, dehydrated through an ethanol and xylene series, embedded in paraffin,
456 and cut into 4-μm sections[49]. After deparaffinization, hematoxylin (FUJIFILM Wako
457 Chemicals) and eosin (FUJIFILM Wako Chemicals) (H&E) staining or ALP activity
458 staining were performed. ALP staining substrates were purchased and used in
459 accordance with the instruction manual (Sigma–Aldrich, St. Louis, MO). The sections
460 were imaged with a Keyence BZ-X800 (Keyence, Osaka, Japan). The shafted hairs
461 were observed using a stereomicroscope (Leica EZ4 HD, Leica, Wetzlar, Germany).

462 ***Statistical analysis***

463 qPCR data are expressed as the mean ± standard error of the mean (SEM) for the fold
464 changes in gene expression compared with that of the control mice. The data were

465 analyzed using one-way ANOVA with multiple comparisons. $p < 0.01$ was considered to

466 indicate statistical significance.

467

468 **Data availability**

469 All data reported in this paper will be provide by corresponding author.

470

471 **Code availability**

472 This paper does not report original code.

473

474 46. Hayashi, K. *et al.* Comparison of sedative effects induced by medetomidine,
475 medetomidine-midazolam and medetomidine-butorphanol in dogs. *J Vet Med Sci*
476 **56**, 951-956 (1994).
477 47. Kawai, S., Takagi, Y., Kaneko, S. & Kurosawa, T. Effect of three types of mixed
478 anesthetic agents alternate to ketamine in mice. *Exp Anim* **60**, 481-487 (2011).
479 48. Klein, R. C. Fire safety recommendations for administration of isoflurane
480 anesthesia in oxygen. *Lab Anim (NY)* **37**, 223-224 (2008).
481 49. Inoue, A. *et al.* VNUT/SLC17A9, a vesicular nucleotide transporter, regulates
482 osteoblast differentiation. *FEBS Open Bio* **10**, 1612-1623 (2020).
483

484

485 **Acknowledgements**

486 The authors thank William N. Addison for comments on the manuscript. This work was

487 supported by Supported by Kitakyushu Foundation for the Advancement of Industry,

Science and Technology (FAIS) 2023 (to S. K.), The YMFG Regional Enterprise Support Foundation 2024 (to S. K.), Suzuken Memorial Foundation 2023 (to S. K.), The Joint Usage/Research Center for Developmental Medicine, IMEG, Kumamoto University (to S. K.).

Author contributions

S.K., K. T., A. W. and K. M. conceived of and designed the study. S.K., A.W., and K. M. are performed experiments. S. K., K. T., M. N., Y. O., O. K., and M. T. analyzed the data. S. K. and O. K. wrote the manuscript.

Competing interests

The authors declare no competing interests.

Additional information

Correspondence and requests for materials should be addressed to Shoichiro Kokabu, D.D.S, Ph.D., Division of Molecular Signaling and Biochemistry, Kyushu Dental University, 2-6-1 Kitakyushu, Manazuru, Kitakyushu, Fukuoka 803-8580, Japan, Telephone: +81-93-285-3047, FAX: +81-93-285-6000; E-mail: r14kokabu@fa.kyu-

506 dent.ac.jp Reprints and permissions information is available at

507 www.nature.com/reprints.

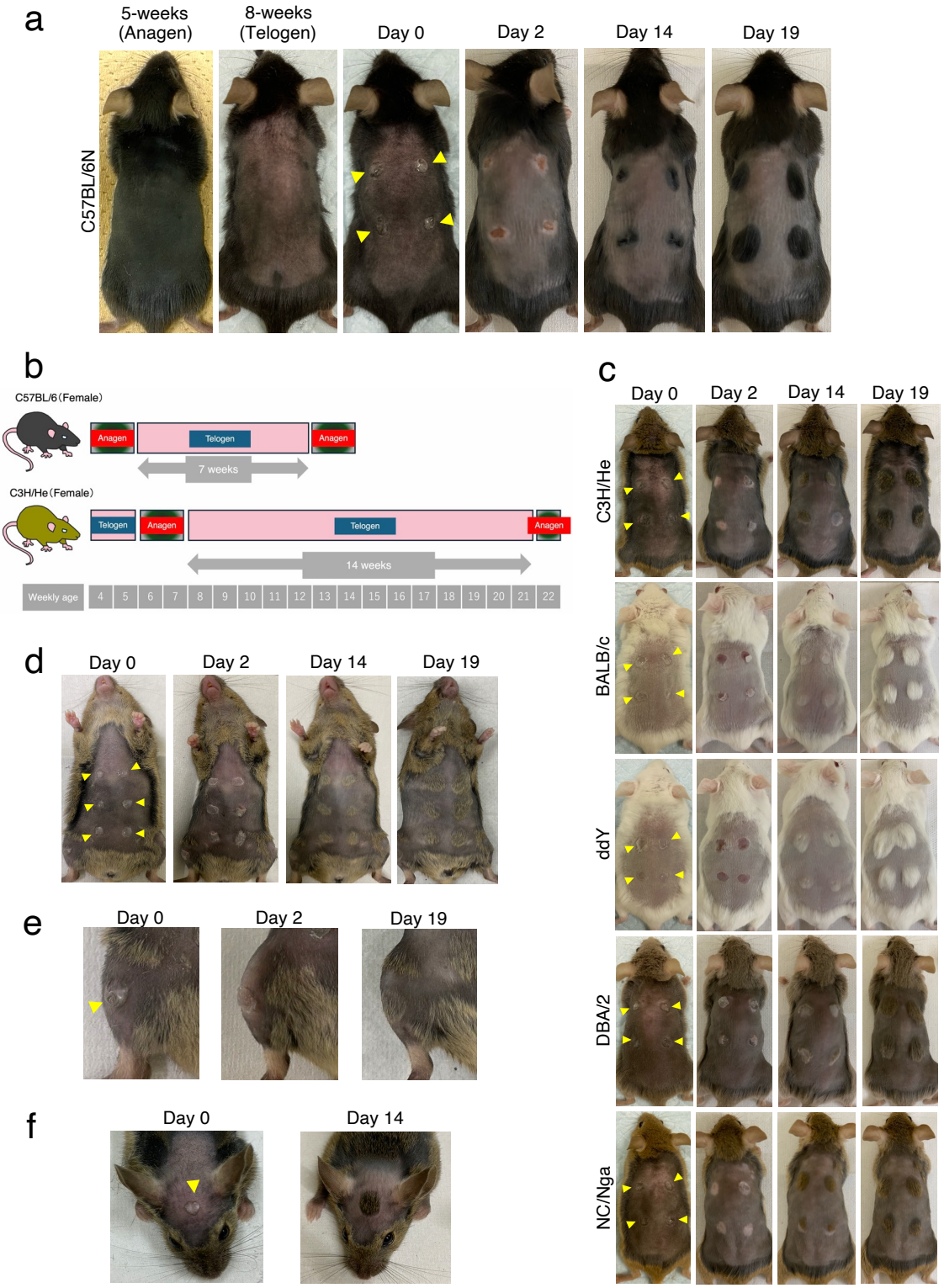

Fig. 1. Pyroxylin induces skin wounds followed by hair regeneration.
(a) Ten percent pyroxylin solution was applied to the dorsal skin of 5- and 8-week-old C57BL/6N female mice after shaving (yellow arrowhead). Representative photos of 5-week-old mice on day 2 and 8-week-old mice on days 0, 2, 14 and 19 after shaving are shown. (b) The schematics represent the hair cycle of C57BL/6N or C3H/He female mice, as previously reported. (c) Pyroxylin was applied to the dorsal skin of 8-week-old C3H/He, BALB/c, ddY, DBA/2, and NC/Nga mice after shaving (yellow arrowhead). Representative photos on days 0, 2, 14, and 19 are shown. (d-f) Pyroxylin was applied to the skin of the abdomen (d), lower leg (e), and head (f) after shaving (yellow arrowhead). Representative photos on days 0, 2, 14, and/or 19 are shown. (a-f) All mice examined exhibited the same trend (n=6).

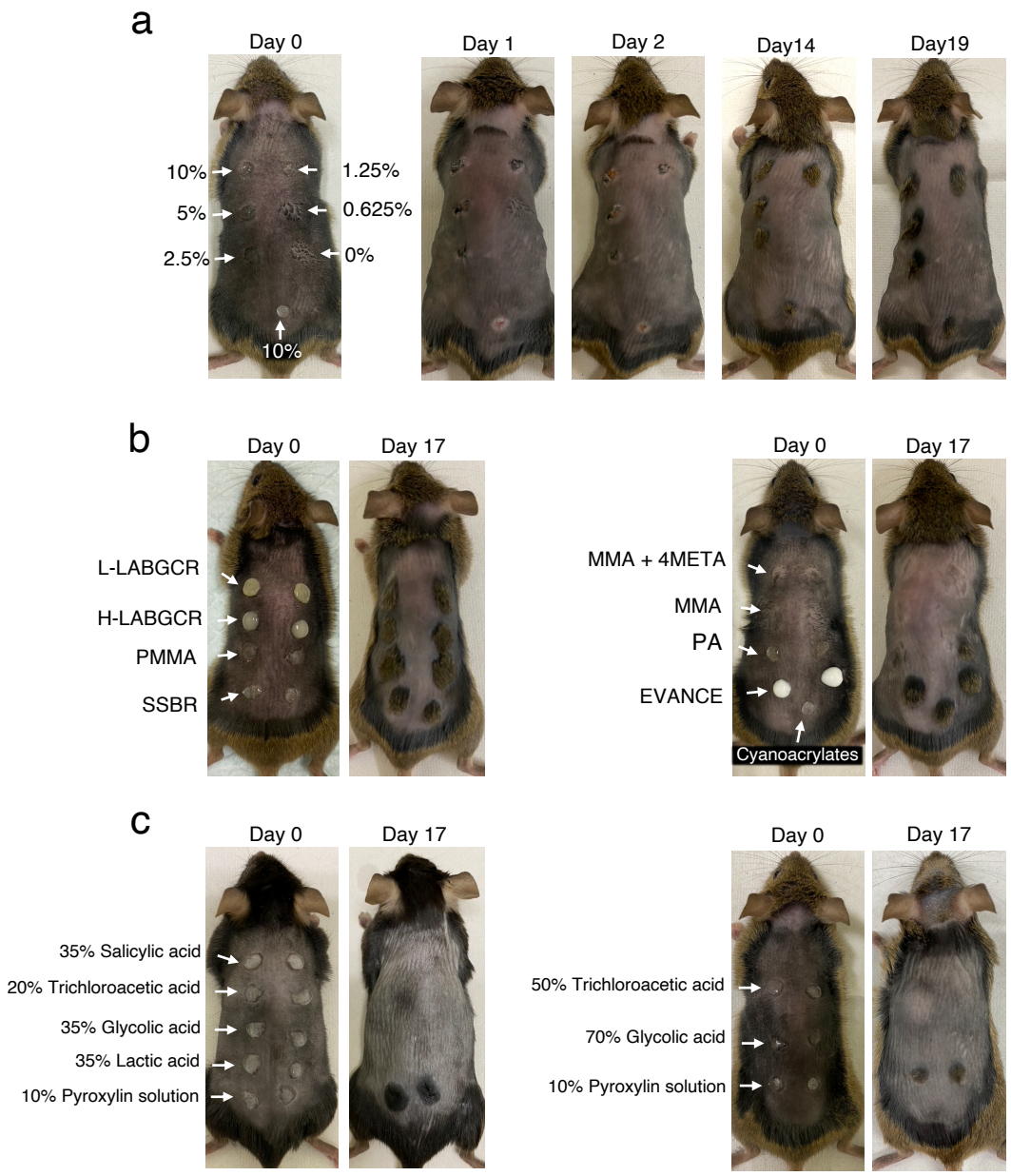

Fig. 2. Hair regeneration is induced in the skin by the application of adhesive and shrinkable materials. (a) Zero (ethanol: diethyl ether = 1:1 weight), 0.625, 1.25, 2.5, 5, or 10% pyroxylin solution was applied (yellow arrowhead) to the dorsal skin of 8-week-old C3H/He mice after shaving. Representative photos on days 0, 2, 14, and 19 are shown. (b and c) Low- or high-shrinkage light-activated Bis-GMA-based composite resins (L-LABGCR or H-LABGCR), PMMA, SSBR, MMA, MMA + 4-META, PA, EVACE, and cyanoacrylates (b). After shaving, 35% salicylic acid solution, 20% or 50% trichloroacetic acid solution, 35% or 70% glycolic acid solution, and 35% lactic acid solution (c) were applied to the dorsal skin. Representative photos of three independent experiments are shown.

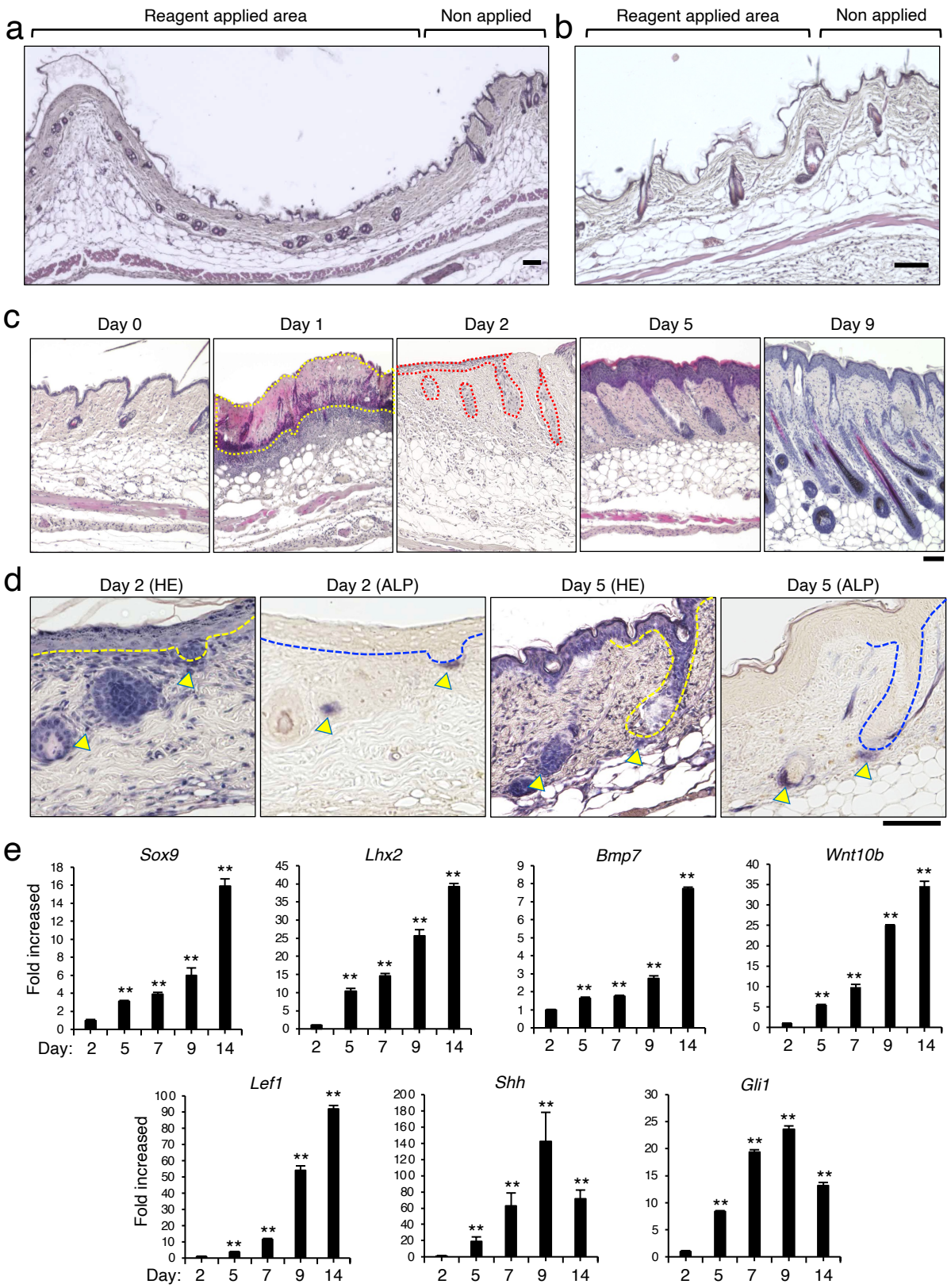

Fig. 3. Hair follicle neogenesis following the separation of the epidermis and dermis.
(a and b) Representative H&E staining images of wounds on dorsal back skin 3 hours after pyroxylin application (a) and a corresponding magnified image (b) are shown. (c) Representative H&E staining images of dorsal back skin wounds on days 0, 1, 2, 5, and 9 are shown. The yellow and red dotted lines indicate the necrotic epidermis and growing panicles, respectively. (d) Representative H&E staining (left) and ALP activity staining (right) images of wounds on the dorsal back skin on days 2 or 5 are shown. The left and right images are consecutive specimens. The arrowhead indicates the ALP activity-positive area. The yellow and blue dotted lines indicate growing panicles and hair follicles, respectively. Representative images (a-d) with the same trend from 6 individual mice are shown. (a-d) Scale bars indicate 100 μm. (e) mRNA levels of Sox9, Lhx2, Bmp7, Wnt10b, Lef1, Shh, and Gli1 in the dorsal back skin of wounds on 2, 5, 7, 9, or 14 were determined by real-time PCR. The data are expressed as the mean ± SEM of triplicate measurements. $^{**}p < 0.01$, compared with the day 2 sample. Essentially, the same results were obtained from three independent mice.

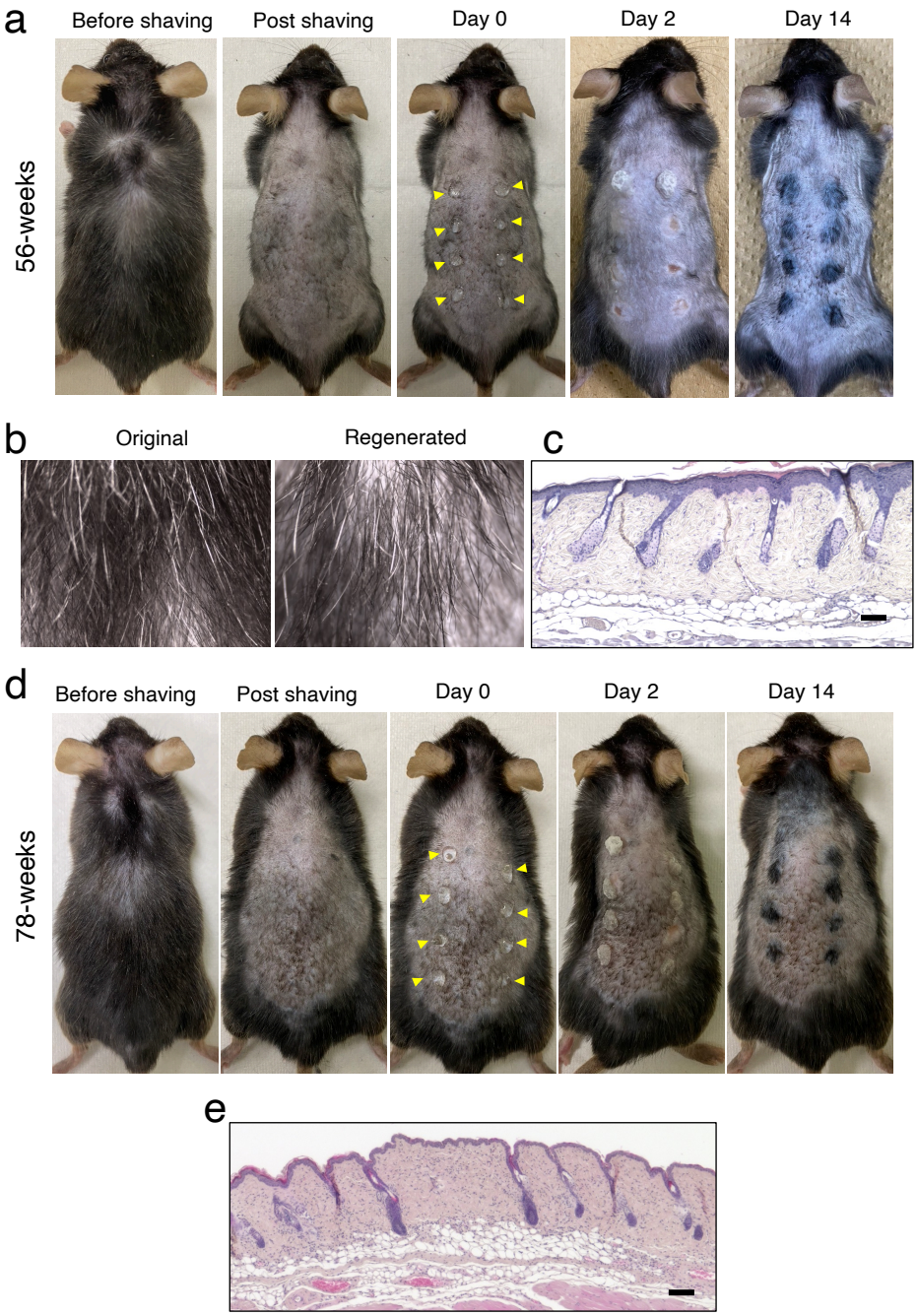

Fig. 4. ESHN in middle-aged and aged mice.
(a-e) Ten percent pyroxylin solution was applied (yellow arrowhead) to the dorsal hair of middle-aged (a-c) and aged (d, e) C57BL/6J male mice after shaving. (a, d) Representative photos on days 0, 2, and 14 are shown. (b, d) Representative photos of original resided hairs (left) and regenerated hairs (right: on day 20) observed under stereomicroscopy are shown. (c, e) Representative H&E staining images of dorsal back skin wounds on day 5 are shown. Scale bars indicate 100 μm. (a-e) All mice examined exhibited the same trend (n=6).

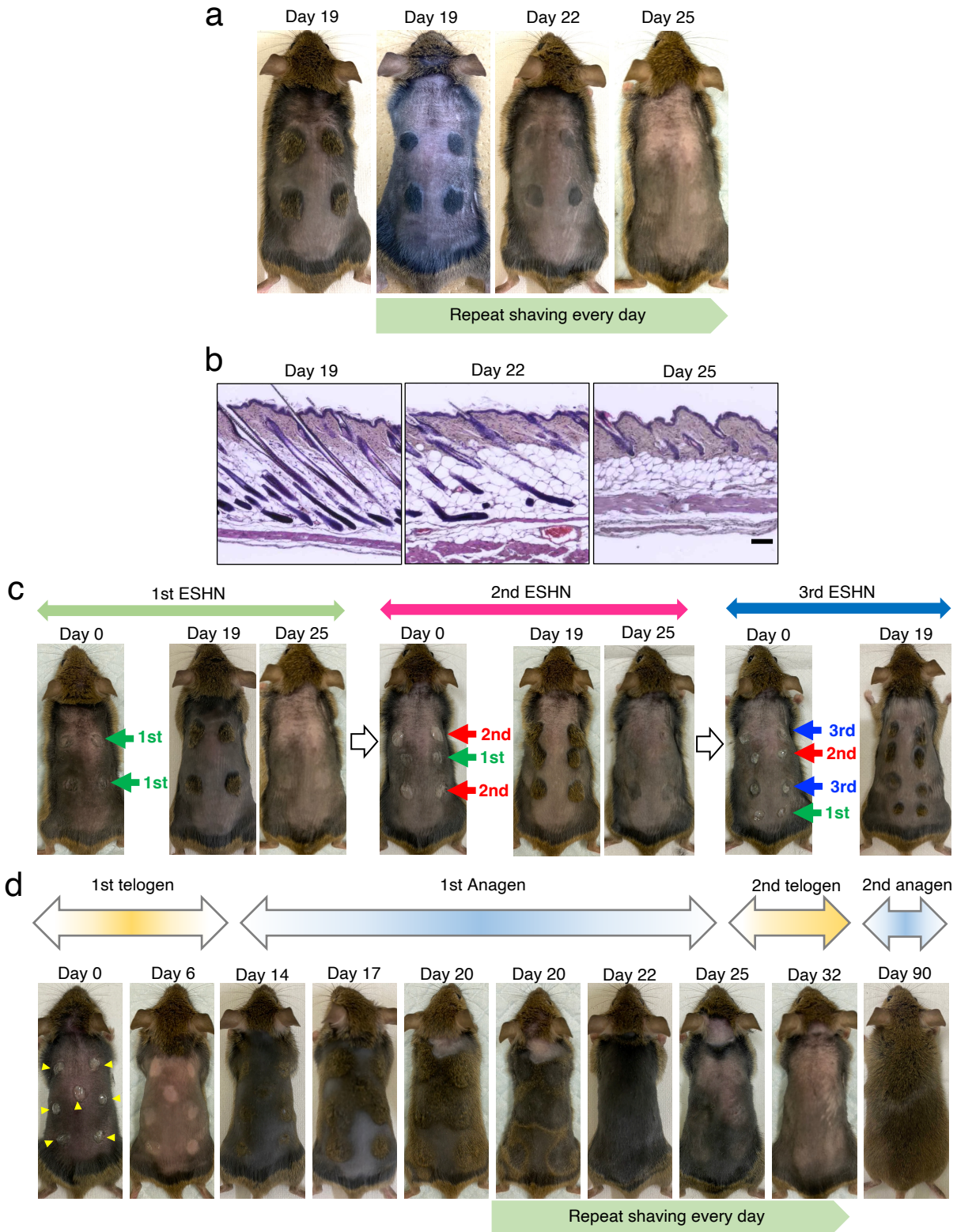

Fig. 5. Hair cycle synchronization in regenerated and surrounding hairs.
(a) Ten percent pyroxylin solution was applied to the dorsal hair of 8-week-old C3H/He mice after shaving. Beginning on day 19, the regenerated hairs were shaved every day. Representative photos on days 19, 22, and 25 are shown. (b) Representative H&E staining images of dorsal back skin wounds on days 19, 22, and 25 are shown. (c) Ten percent pyroxylin solution was applied to the dorsal hair of 8-week-old C3H/He mice after shaving (green arrow). The photos are shown on day 0, 19, or 25 (1st ESHN). A 10% pyroxylin solution was also applied at the same location for the first time (2nd time; red arrow). The photos are shown on day 0, 19, or 25 (2nd ESHN). Again, a 10% pyroxylin solution was applied to the same place for the 2nd time (3rd time; blue arrow). The photos are shown on day 0, 19, or 25 (3rd ESHN). (d) Pyroxylin was applied to the dorsal hair of 4-week-old C3H/He mice after shaving (yellow arrowhead). Beginning on day 20, the regenerated hair was shaved every day for 2 weeks. Representative photos on days 0, 6, 14, 17, 20, 22, 25, 32, and 90 are shown. All mice examined exhibited the same trend (n=6).